European Rotorcraft Forum

INVESTIGATING POWER BENEFITS FOR A HELICOPTER BY VARIATION OF THE ANTI-TORQUE DEVICE

Maximilian Mindt, Susanne Seher-Weiß
German Aerospace Center (DLR), Institute of Flight Systems
Braunschweig, Germany

With the usage of electrically driven devices, the rigid connection between main rotor and tail rotor can be broken up, allowing for a tail section that can possibly be optimized for different operating conditions. This paper presents the results of a study investigating the power benefits of different variations of the electric anti-torque device. The investigations were performed using an engineering model of a main rotor - tail rotor helicopter built up in the Versatile Aeromechanics Simulation Tool (VAST). The studied variations include horizontal and vertical tilting of the tail rotor, changing tail rotor speed and fin angle as well as fin size and geometry. Various flight conditions such as hover, forward flight, quartering flight, climb, and descent have been investigated. The largest power benefits were observed for (1) a combination of reduced tail rotor speed and a fin angle varying between $12\,\mathrm{deg}$ for low speed forward flight and $6\,\mathrm{deg}$ for high flight speeds and (2) an increased fin area with the tail rotor being shut off for flight speeds above $35\,\mathrm{m/s}$.

Symbols

A	area, m^2
b	fin height, m
F	force, N
M	moment, Nm
P	power, $\mathrm{Nm/s}$
R	radius, m
V	airspeed, $\mathrm{m/s}$
α	angle of attack, deg
$\alpha_{C_L=0}$	airfoil angle of zero lift, deg
β_{1c}, β_{1s}	tail rotor flapping angles, deg
γ	flight path angle, deg
η	deflection angle, deg
θ_0	collective control angle, deg
θ_c, θ_s	lateral and longitudinal control angles, deg
θ_{TR}	tail rotor collective control angle, deg
Φ, Θ, Ψ	Euler angles (roll, pitch, yaw angles), deg
Ω	rotor speed, rad/s

Acronyms and Indices

DLR	German Aerospace Center
DoF	degree of freedom
fin	vertical tail plane/fin
hor	horizontal
MBS	multibody system
MR	main rotor
TR	tail rotor
VAST	Versatile Aeromechanics Simulation Tool
vert	vertical
0	reference configuration

1. INTRODUCTION

For a main rotor - tail rotor helicopter, the tail rotor is essential for its operation as it counteracts the main rotor torque and thus enables low velocity operations and hovering. The power consumed by the tail rotor does not contribute to the upward or forward thrust and is therefore seen as a necessary but wasted power contribution. The tail rotor's ability to contribute upward thrust via tilting of the rotor has already been used for example in the famous Black Hawk (UH60) helicopter [1]. Rozhdestvenskiy and Vaintrub made detailed investigations for possible retrofits of the Mi8 and Mi24 helicopters with a vertically tilted rotor in [2].

Within the project eTail, which is funded by the Federal Ministry for Economic Affairs and Climate Action, the replacement of the helicopter tail section by an electric yaw moment compensation is investigated. Breaking the rigid connection between helicopter main gear box and tail rotor extends the design space, because the rotational speed of the tail rotor is no longer a fixed ratio of the main rotor speed, enabling flight state dependent settings. There are multiple further possibilities to use

the opened design space, like the rotor matrix approach of United States patent US10526085 [3] that was realized in the EDAT system on a Bell 429 helicopter demonstrator. This and other solutions are discussed in the paper "Full Electric Helicopter Anti-Torque" [4]. That paper also highlights other benefits to be expected from an electric tail section, while the paper at hand investigates the benefits of different variations of tail rotor and vertical fin settings with respect to power benefits.

2. METHOD OF INVESTIGATION

The case study focuses on a practical application to the AW09 helicopter currently undergoing the certification process. This helicopter features a five bladed main rotor and a ten bladed tail rotor integrated in a shroud, as shown in Figure 1. To assess the power requirements of

Figure 1: A prototype of the AW09 helicopter during flight testing [5]

the various design options, different variants of an engineering model of the AW09 are compared. The models are built up in VAST, the Versatile Aeromechanics Simulation Tool [6], which is currently under development at the German Aerospace Center (DLR).

Though only the tail section is changed, the focus is given to the helicopter overall power requirements rather than the tail rotor power consumption during the investigations. Otherwise it would be easily possible to misjudge the benefits of a change. For example, when the tail rotor is covered inside a closed shroud and not rotating, it will not contribute to the power, leading to a reduction of 100% for this component. The counteraction of main rotor torque will have to be provided by other components, leading to an increase in power consumption due to those other components, though. The total required power then may be bigger or smaller than the reference configuration, depending on the split of power contributions. It also has to be kept in mind that the tail rotor contributes to 9.5% of the total power required for hovering in standard atmosphere condition at sea level, and less in forward flight. Hence, the maximum overall power benefits are expected to stay below these reference power shares.

All relevant flight states have to be considered in the investigations in order to give a realistic picture of the influences of design changes. This means not only steady horizontal flight conditions, but also hover, climb and descent as well as quartering flights have to be considered. Changes in center of gravity, influences on the control system and others have to be monitored in parallel to identify side effects that may prevent a practical application.

3. MODEL DESCRIPTION

In the VAST models, the structural dynamics are represented by a multibody system (MBS) with rigid bodies. The fuselage body features a six degree of freedom (DoF) joint to allow for a free movement in space. A joint driven about the vertical axis provides the rotational speed to the rotor head, which features the connection points for the main rotor blades. All five rotor blades are connected to the hub via joints in flap-lag sequence, succeeded by a third joint which is driven by the blade pitch angles provided from the swashplate model. The latter only facilitates the transfer from pilot controls to the single blade pitch settings, no structural kinematics are considered.

The fuselage also has an attachment point for the tail rotor. Since a very complex flow field changing with operational conditions is expected for the shrouded tail rotor, a dedicated modeling effort is needed for this single component to accurately capture its behavior. The qualitative variation with operating condition was also shown by numerical simulation in Ref. [7]. While the detailed flow phenomena are difficult to match even with CFD, the basic aerodynamic behavior might be modeled in a computationally efficient way suited for inclusion into a comprehensive tool as VAST in the future. For the preliminary investigations conducted in the present research, the tail rotor is treated as an open rotor. Nevertheless, two models of different complexity were investigated. In the simple version, the tail rotor attachment point serves as interface for the comprehensive tail rotor model derived by Padfield [8], but with the velocity components completely provided via the MBS. In a more detailed version, a driven joint provides the tail rotor rotational speed to the tail rotor hub, where each of the ten blades are connected via a driven joint that imposes the blade pitch setting. The aerodynamics of the tail rotor are modeled with the same sophistication as the main rotor.

Table look up polars of the employed airfoils are used for blade element aerodynamics of the rotor(s), taking into account chord variation effects for the tapered blade tip. The downwash is calculated with the model by Pitt and Peters [9] for the main rotor and the simpler Glauert model [10] for the tail rotor. The main rotor blades are discretized into 10 aerodynamic sections such that each section covers the same rotor area during a revolution. The empennage loads are calculated based on polar air-

loads models that use a single comprehensive polar for a whole component, e.g. the fin. The respective polars are generated based on the airfoils incorporated for the component, considering a lift efficiency factor for three-dimensional flow effects. For the fuselage loads, an existing polar available for the Bo105 helicopter was scaled according to the estimated drag surface.

Figure 2 shows a comparison of the simple model variant with tail rotor after Padfield and the full-MBS variant with discrete aerodynamics. The main difference is an offset in tail rotor pitch θ_{TR}, seen in the upper left plot for the purple lines. This can be attributed to the Padfield model working with a linear lift curve slope without zero lift angle offset $\alpha_{C_L=0}$, whereas the airfoil data used in the complex model feature a $\alpha_{C_L=0}$ of $-3\,\mathrm{deg}$ to $-4\,\mathrm{deg}$. Additionally, the Padfield model features a delta-3 effect which increases the required θ_{TR}. Due to the quadratic drag polar, the higher α needed for the same lift also leads to a higher power consumption as shown in the lower right plot. Overall, the match between the variants is quite good. Therefore, the simpler model was used for the parameter variations as it is computationally less expensive.

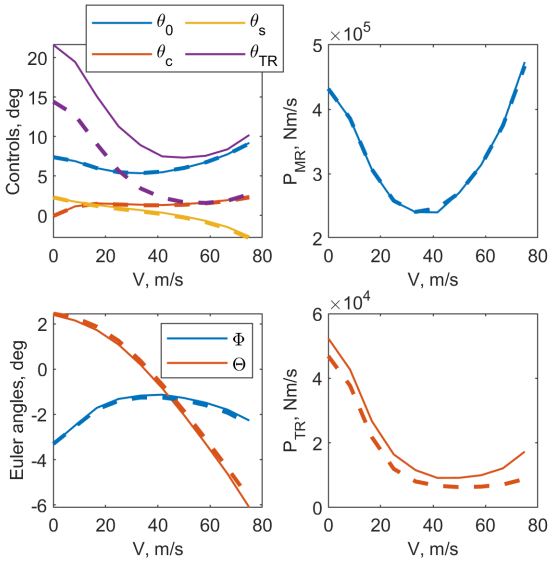

Figure 2: Comparison of power, controls and attitude angles for the full-MBS model (dashed line) and the simple variant

4. HORIZONTAL AND VERTICAL TILT

In a first step, the benefits of tilted tail rotors are investigated using the simple Padfield model of an open tail rotor for trimmed forward flight condition. The definition of the horizontal tilt angle η_{hor} and the vertical tilt angle η_{vert} of the tail rotor as well as the fin angle η_{fin} can be seen in Figure 3.

Figure 4 shows that a vertical tilting of the tail rotor can lead to total power savings especially in hover and low

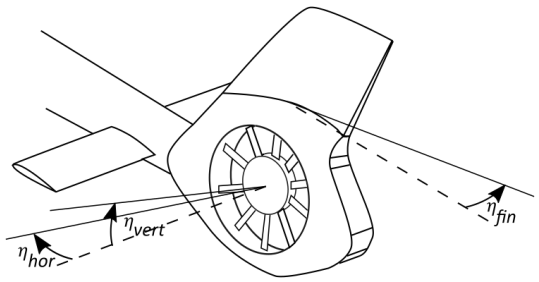

Figure 3: Definition of horizontal tilt angle η_{hor}, vertical tilt angle η_{vert} and fin angle η_{fin}

forward velocity flight conditions, which are shown with blue and orange lines, respectively. The ratio of total power needed for the modified configuration P to the total power P_0 of the reference configuration at that velocity is depicted in the figure. The maximum power savings amount to 1.8% for a tilt angle of $25\,\mathrm{deg}$ at a flight speed of $8.33\,\mathrm{m/s}$. To put that into perspective, the unaltered tail rotor contributed 8.9% to the total power, so this means a reduction of 20% in power required for the anti-torque.

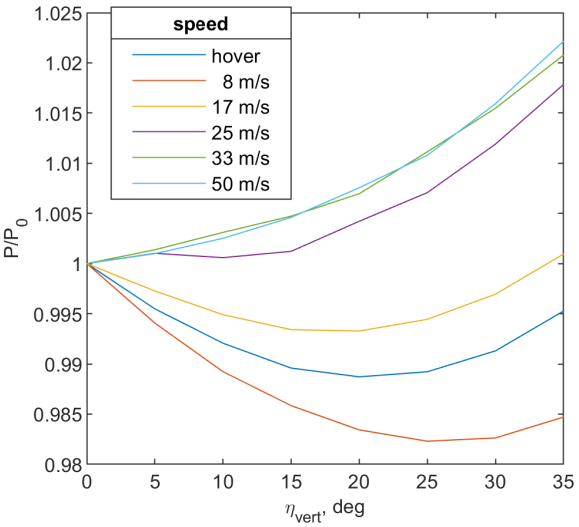

Figure 4: Change in power for variation of vertical tilt angle

As a side-effect, the upwards thrust component at the tail creates a negative pitching moment that counters effects of a shift of the center of gravity to the back. This shift is expected with installation of an electric motor at the tail due to the additional component. The simulations showed a much larger influence on the pitch equilibrium than needed to cancel out the effect of the center of gravity shift, though. In Figure 5, the changes in trim values are shown from hover to maximum forward speed of $75\,\mathrm{m/s}$. The trim values of the controls θ_0 and θ_c as well as the roll angle are not shown because the changes there are marginal compared to the ones shown. In the upper right plot of Figure 5 it can be seen that the he-

licopter pitch angle Θ gets negative in hover at 20° of tail rotor tilt. The longitudinal control θ_s shown on the lower left, also increases drastically and could exceed the swashplate limits for high tilt angles. These findings mirror the problems identified by Rozhdestvenskiy and Vaintrub in [2] for the inclusion of a tilted rotor in already existing helicopter models. Because of other effects influencing the helicopter operation like a yaw-pitch-coupling in control this design change was discarded for the further investigations.

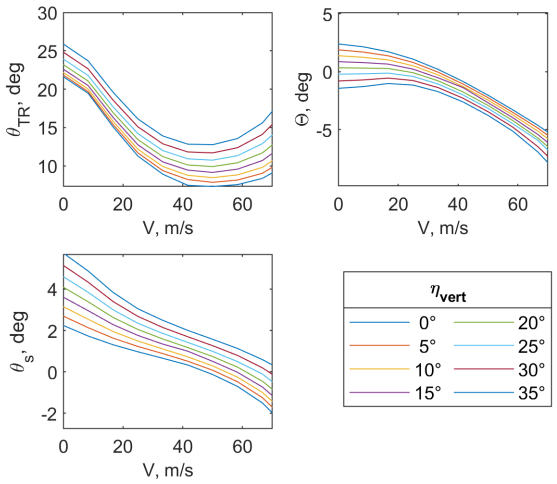

Figure 5: Change in trim controls and attitude angles for variation of vertical tilt angle

A horizontal tilting was found to have a negative influence on power required except for a slight decrease at fast forward flight of $75\,\mathrm{m/s}$, with the optimum just giving 0.5% power savings at a tilting of 55° as shown in Figure 6. Since this configuration requires much more power at all lower flight velocities or would not even be trimmable with a realistic rotor model (without linear lift curve slope), a steering mechanism would have to be constructed just for this small improvement at the edge of the envelope. Therefore, tilting the tail rotor in horizontal direction was also discarded.

5. VARIATION OF TAIL ROTOR SPEED AND FIN ANGLE

For an electrically driven tail rotor, the tail rotor speed is no longer coupled to the main rotor speed via a fixed gear transmission ratio. Therefore, it was investigated whether the overall power consumption of the helicopter can be reduced by adapting the tail rotor speed to the different flight conditions. Investigations for the UH60A [11] led to a 30% reduction in tail rotor power in forward flight by using an optimized tail rotor speed.

With sufficient airflow as present in forward flight a rudder can generate forces that counteract the main rotor torque. For simplicity, instead of implementing a separate rudder surface, the whole fin was deflected. This fin deflection was first investigated separately and later also in combination with varying tail rotor speed.

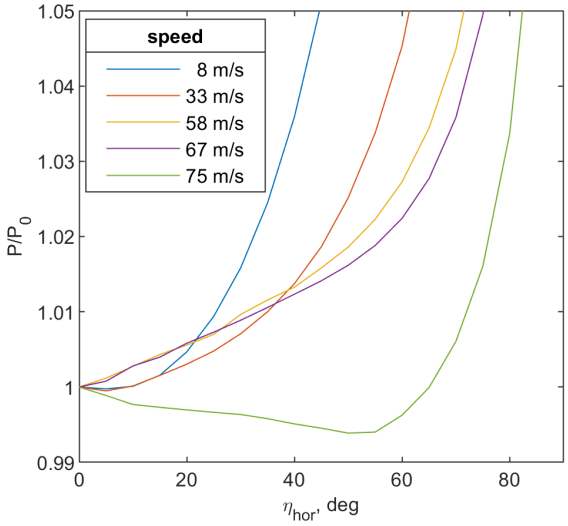

Figure 6: Change in power for variation of horizontal tilt angle

5.1. Variation of Tail Rotor Speed

Within the implementation of the simplified Padfield tail rotor model in VAST, tail rotor speed is not specified directly but only as the ratio between tail rotor and main rotor speed (Ω_{TR}/Ω_{MR}). For the reference case of the unmodified AW09, this ratio is close to seven. To investigate the effect of different tail rotor speeds, the speed ratio Ω_{TR}/Ω_{MR} was varied between 2 and 14.

Figure 7 shows the change in trim values as a function of the speed ratio. Reduced tail rotor speeds are shown with solid lines and increased speeds with dashed lines. Changing the tail rotor speed has hardly any influence on the main rotor controls and attitude angles which is why they are not shown in Figure 7. Reducing the tail rotor speed leads to a larger collective and larger flapping angles β_{1c} and β_{1s} at the tail rotor. Flap angles are calculated here because the applied simplified tail rotor model uses a central flapping hinge with delta-3 effect. The decreased Ω_{TR} decreases the rotational inertial forces which tend to keep the blades straight as well, leading to a higher influence of the aerodynamic forces and thus higher flapping angles. As a ducted tail rotor has no flapping hinge, angles larger than $7\,\mathrm{deg}$ which are reached for a speed ratio of 4 are assumed as not representative for the system under consideration. Aside from that, the Padfield tail rotor model uses a linear lift curve slope without stall, leading to arbitrarily high trimmed θ_{TR} values. As can be seen in the upper left plot of Figure 7, the low velocity flight trim results for tail rotor pitch are unrealistically high for $\Omega_{TR}/\Omega_{MR} = 4$ and 5.

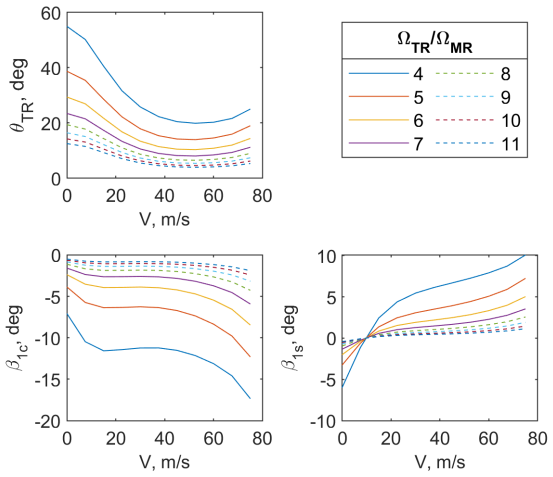

Figure 7: Trim values as a function of speed ratio

The overall power as a function of the speed ratio is shown in Figure 8. As before, the power values are referred to the power of the current AW09 as the reference configuration, thus the ratio P/P_0 is shown. The data in the upper right part of the plot was removed for combinations where the blade tip speed at the advancing side of the rotor would reach the speed of sound. The results close to that border are of course also straining the application range of the model.

The speed ratio of the reference configuration is optimal for small and intermediate speeds. For higher speeds ($V \geq 60\,\mathrm{m/s}$) a reduction in power - up to 1% at $75\,\mathrm{m/s}$, which corresponds to one third of tail rotor power - can be achieved for slightly elevated tail rotor speeds.

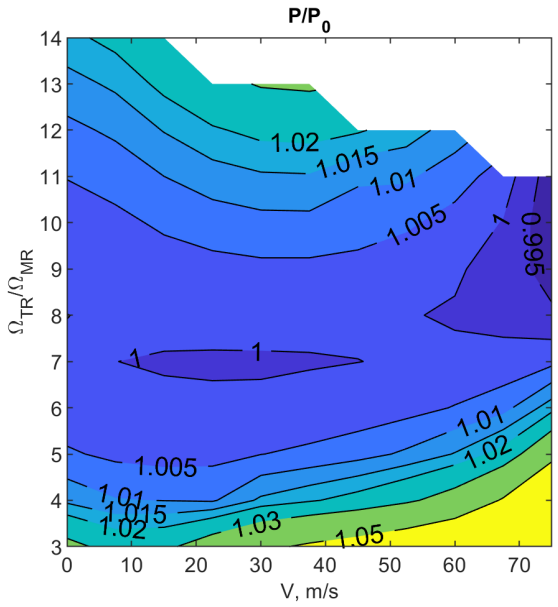

Figure 8: Change in power for varying tail rotor speed

5.2. Variation of Fin Deflection

For small flight speeds, the fin deflection η_{fin} has no influence on the trim values of the controls because the dynamic pressure is too small to generate a significant side force. Starting at a speed of about $20\,\mathrm{m/s}$ a fin deflection leads to a reduced tail rotor collective trim. Due to the proximity of tail rotor and fin and the main force contribution of both being the side force, the influence of fin deflection on the overall trim, namely the main rotor control angles and the attitude angles is negligible.

Figure 9 shows the change in overall power as a function of the fin deflection for fin angles up to $\eta_{fin} = 25\,\mathrm{deg}$. The power values are referred to the case without fin deflection, $P_0 = P(\eta_{fin} = 0\,\mathrm{deg})$. For velocities above $25\,\mathrm{m/s}$ a fin angle in the region of 7 to 12 degrees yields a power saving of 1 to 1.5%. At high fin deflections, the fin generates more sideward thrust than necessary. Therefore, the tail rotor has to generate a counteracting thrust. Additionally, the fin stalls, entailing higher drag which has to be countered by additional forward thrust of the main rotor. Overall, more power is thus required.

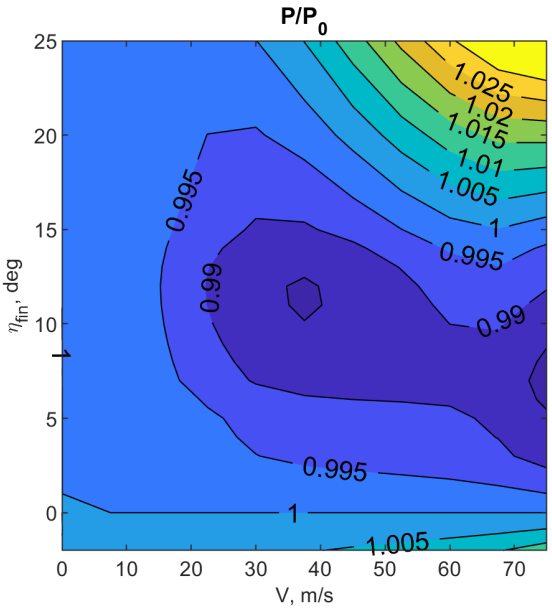

Figure 9: Change in power for varying fin angle

5.3. Combined Variation

Next, tail rotor speed and fin angle were varied in combination. For rotor speed, mainly reductions with respect to the reference value were considered. Results for rotor speed ratios below 4 could only be calculated for flight speeds above $30\,\mathrm{m/s}$. The fin angle was again varied over the range of 0 to $15\,\mathrm{deg}$.

The change in overall power with respect to the reference configuration is shown in Figure 10 for all forward velocities. For velocities below $30\,\mathrm{m/s}$ the optimal tail ro-

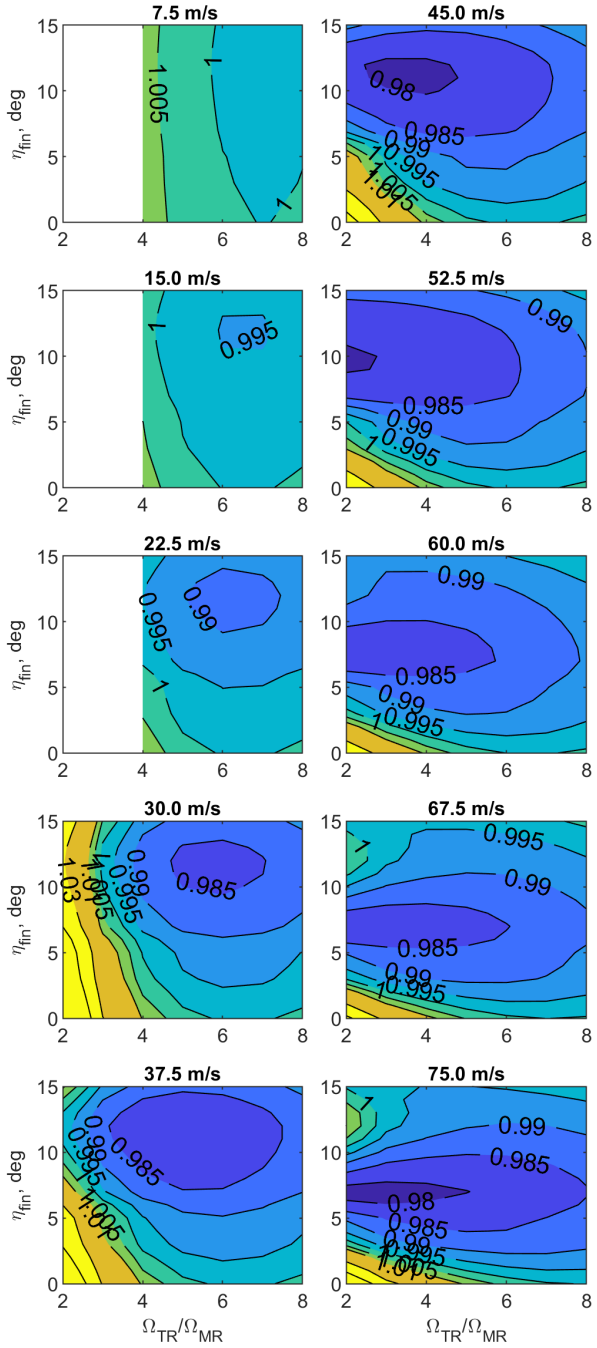

Figure 10: Change in power for variation of rotor speed and fin angle

tor speed is close to the reference value and the optimal fin angle is $12\,\mathrm{deg}$. For increasing flight speed, the optimum moves towards lower rotor speeds and a fin angle of $7\,\mathrm{deg}$. This is especially interesting because for the sole variation of the rotor speed shown in section 5.1, going below the reference rotor speed led to an increased power consumption. With the additional side force of the inclined fin in the combined variation, the tail rotor can be unloaded and operated at low rotor speed and pitch angle, leading to the beneficial effect. The maximum achievable power saving is about 2.2%. This is equal to 77% of the power the tail rotor needs at the according flight speed of $75\,\mathrm{m/s}$ for the reference configuration.

5.4. Shutting off the Tail Rotor

So far, the power optimum in forward flight above $50\,\mathrm{m/s}$ was at the lowest investigated tail rotor speeds, but the simple tail rotor model did not allow to trim at lower speed ratios. To explore potential further power benefits by shutting off the tail rotor in forward flight, the tail rotor model was removed entirely from the calculations. This configuration change can be seen as representative because the rotor inside the shroud will be subjected to only a fraction of the oncoming flow due to the flight speed if it is not rotating. This would be even more true if the shroud was closed off by a shutter. This setup is of course only trimmable when a certain flight speed is reached and the yaw moment can be canceled by the fin.

An additional power saving can be achieved compared to a configuration with the same fin angle but the tail rotor being used in the trim. This is going to be illustrated in section 7.

6. FIN SIZE VARIATION

According to investigations reported in Ref. [12], an additional aerodynamic surface the size of 2% of the main rotor area with a lever arm equivalent to the rotor radius is sufficient to fully counteract the main rotor torque in forward flight. The simplest way of realizing such an additional surface is increasing the size of the vertical tail.

For an approximate investigation of the influence of vertical fin size, it was assumed that the aerodynamic properties of the fin do not change fundamentally when scaling the fin area. Thus the correction factors for mounting and 3D-effects were not changed. The fin loads are calculated by the polar model introduced in section 3. This model has the component reference area as an input parameter which is thus the only parameter to be modified for the fin size variation.

The fin area A_{fin} was varied in the range of $100 - 170\%$ of the reference fin area $A_{fin,0}$ for the investigation. As can be seen in Figure 11, the trim value of the tail rotor collective decreases with increasing fin area and for an increase of the fin size to 160% of the reference value

even counteracting thrust is necessary in fast forward flight. Figure 11 shows that unlike for the variation of tail rotor speed, the flap angles stay well inside the bounds deemed acceptable for the model.

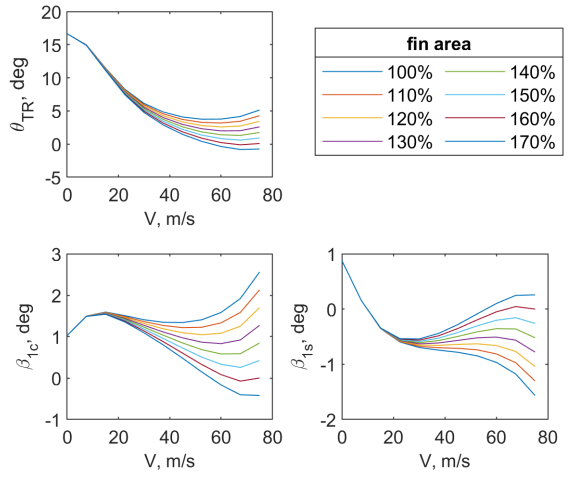

Figure 11: Trim values as a function of fin area

The corresponding change in overall power is shown in Figure 12. For the maximum airspeed of $75\,\mathrm{m/s}$, an increase of the fin area to $150-160\%$ saves about 1% in overall power. Note that at high velocities, with the biggest fin sizes there is still a power saving very close to the optimum despite the tail rotor starting to counteract the fin force. This is due to the very low thrust needed, which keeps the tail rotor airfoils at low drag, summing up to a lower power consumption than in the reference case.

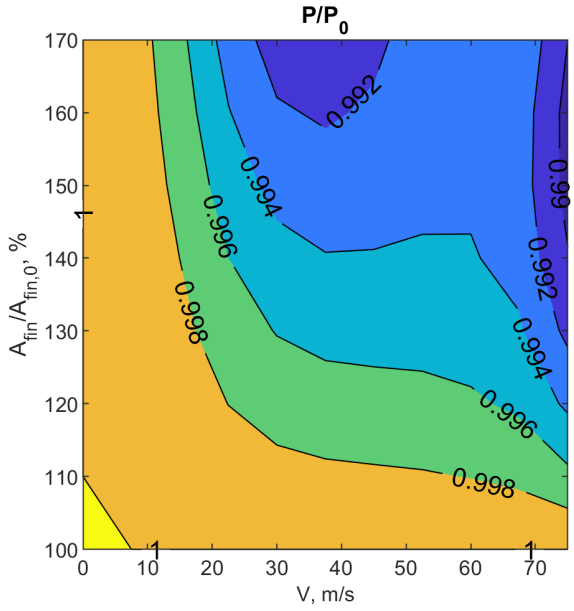

Figure 12: Change in power for increasing fin area

6.1. Trim via Tail Rotor Speed

For an electrically driven tail rotor, the thrust can not only be varied by changing the tail rotor collective control angle Θ_{TR} but also by changing the tail rotor speed Ω_{TR}. The implementation of an option to trim via tail rotor speed is different for the MBS model and the model with the simple tail rotor. The detailed MBS model already contains a joint with rotational speed specification. This speed can be defined as a control variable for trim. As mentioned in the preceding section on rotor speed variation, tail rotor speed was not directly available in the simple model but only indirectly as the ratio with respect to main rotor speed. Thus, an option to specify tail rotor speed directly had to first be implemented in the model. Then the VAST solver had to be given access to this variable to be able to use it as a control variable.

As the helicopter still has six degrees-of-freedom, one other parameter has to be fixed when trim is to be achieved via tail rotor speed to still have a unique trim problem. Therefore, the tail rotor collective angle was fixed for trimming via tail rotor speed. An example comparing the two trim variants can be found in Ref. [4].

The investigations with respect to fin size variation were then also conducted using tail rotor speed instead of tail rotor collective for trim. The results showed comparable power savings as those obtained with the conventional trim using tail rotor collective.

7. INFLUENCE ON NORMAL OPERATION

The preceding investigations have shown that an increased fin size leads to power savings and even allows to shut off the tail rotor altogether in cruise flight. Therefore, a configuration with a fin size of $1\,\mathrm{m}^2$, more than doubling the original size, was chosen for investigating the influence of an enlarged fin on normal operations such as cruise flight, climb and descent, and quartering flight. The goal was to identify possible drawbacks of the design changes like reduced operability in sideward wind hover conditions as they appear in alpine rescue missions. The aspect ratio was not yet fixed but was allowed to vary. To better capture the effect of changes in fin geometry, the generation of polars based on the airfoil properties was extended to include the influence of aspect ratio on induced drag as known from airfoil theory, e.g., Schlichting and Truckenbrodts textbook chapter 7 [13].

7.1. Level Flight

Figure 13 shows the power change with respect to the current AW09 in level flight. The power saving is larger for the more slender fin with a height of $b = 1.6\,\mathrm{m}$ as the increased aspect ratio reduces the induced drag. For speeds above $35\,\mathrm{m/s}$ the tail rotor can be shut off which

yields approximately another 1% reduction in power compared to the same configuration with the tail rotor still running.

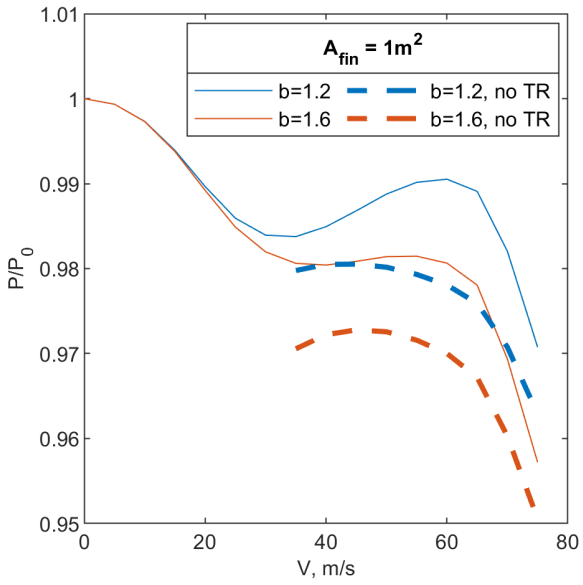

Figure 13: Power change in level flight

7.2. Climb/Descent

In climb close to the velocity of maximum endurance, the larger fin leads to a power reduction of 1.5% and 1.8%, respectively, as shown for positive flight path angles γ in Figure 14. Interestingly, the benefits are almost constant for the different climb angles.

With increasing descent angle, the power benefits of the larger fins are reducing and in steep descent flight ($\gamma < -10\,\mathrm{deg}$), the models with larger fins even need more power than the reference configuration (left part of Figure 14). This can be explained with the following effect: With increasing descent velocity, the fuselage drag contributes more and more to the upward force, thus lowering the thrust needed by the main rotor. This lower thrust is accompanied by a decrease in main rotor torque, which in turn lowers the sideward force to be provided by the tail section. As discussed in the previous subsection, the fins of increased size are able to counteract the torque without the help of the tail rotor at level forward flight of $35\,\mathrm{m/s}$. Due to the decrease of required side force in descent, the larger fins even produce too much sideward force, which the tail rotor needs to counteract. This of course leads to an increase in the power consumption of the tail rotor and thus to an increase in the overall power. Despite the relatively large increase of up to over 6%, the absolute power requirement is still way below the level flight values, so this is not as much of a concern as it seems on the relative scale.

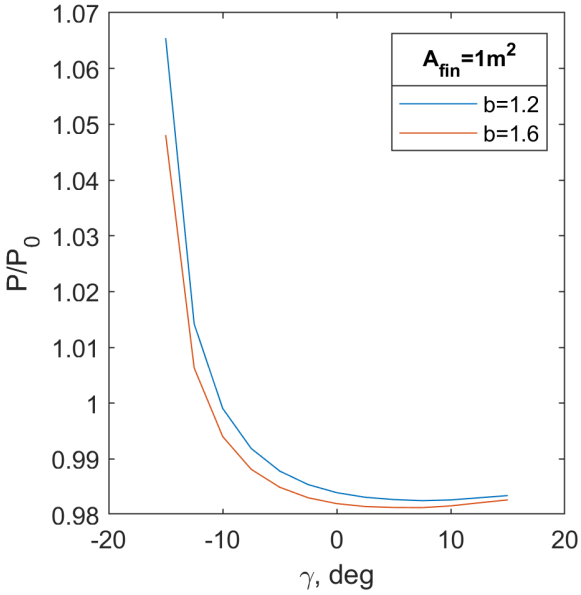

Figure 14: Power change in climb and descent ($30\,\mathrm{m/s}$)

7.3. Quartering Flight

In quartering flight to the right, the high drag of the fin at around 90 degrees angle of attack contributes a sideward force that counteracts the main rotor yaw moment, enabling an unloading of the tail rotor. This leads to a reduction in power required relative to the reference configuration, as shown in Figure 15 for positive velocities. There is essentially no difference between the geometry variants with $1\,\mathrm{m}^2$ of fin area.

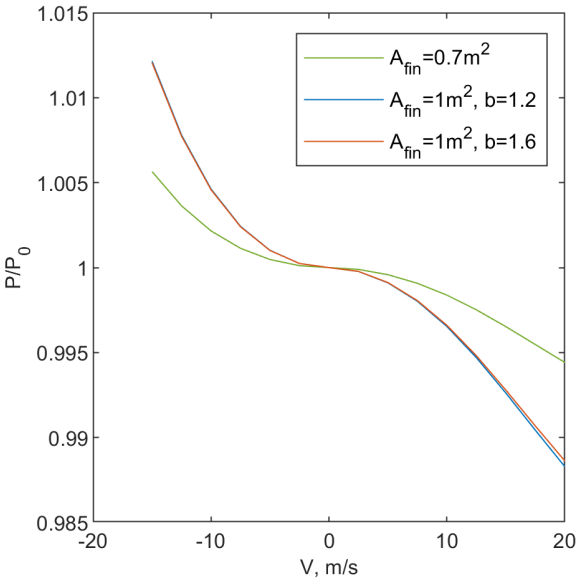

Figure 15: Power change in quartering flight

For flights to the left, the fin drag additionally has to be countered by the tail rotor, leading to increased power

values shown for negative velocities. Nevertheless, quartering flight to the left is still possible for speeds up to $15\,\mathrm{m/s}$. No reduction of the flight envelope with respect to the reference configuration is observed.

It has to be noted that the tail rotor model of Padfield does not cover descents into the vortex ring state in its formulation. Assuming that the normal operating condition formulae can be used for up to a descent velocity (in the tail rotor frame) of half the hover induced velocity, the maximum investigated sideward flight of $20\,\mathrm{m/s}$ only touches that boundary.

8. CONCLUSION AND OUTLOOK

Trim calculations were performed for different variants of the AW09 tail section. The calculations were carried out with engineering models in the comprehensive tool VAST, which is currently under development at DLR. A vertical tilting of the tail rotor was shown to be beneficial for hover and low speed forward flight. Due to implications for the control system and a relatively complex implementation with a shrouded rotor, it seems difficult to apply this change to an already existing helicopter. Tilting the rotor horizontally in the direction of flight was found to be counterproductive except for the highest investigated flight speed.

Variation of the tail rotor speed resulted in small power savings for increased Ω_{TR} at high flight speeds. A reduced rotor speed increased the required total power. The opposite of this was found for the combined variation of fin installation angle and rotor speed. With an apparent η_{fin}, the tail rotor can be unloaded and the needed thrust can be generated at advantageous conditions for lower Ω_{TR}. Since the optimal fin angle is decreasing with flight speed, a steerable fin is advisable.

Alternatively to the variation of fin angle, the increase of the fin size is an option to unload the tail rotor. Investigations with different fin sizes showed that the tail rotor can be fully unloaded for forward flight speeds of $35\,\mathrm{m/s}$ and higher with an increase of the fin area to $1\,\mathrm{m}^2$. As expected, a slenderer fin leads to a more efficient helicopter. Additional power savings were observed when the tail rotor was removed from the simulation, corresponding to shutting off the rotor and enclosing it inside the shroud.

Investigating climb, descent and quartering flight conditions revealed that the optimal variants for hover and forward flight can require more power than the reference configuration in other flight conditions. However, no reduction of the flight envelope was encountered for the modified variants. The overall benefit of the changes has to be assessed based on the envisioned mission profiles. Additionally, the technical feasibility has to be taken into account. Aspects of design requirements and the technical realization for the investigated tail section changes are detailed in the companion paper [4].

As stated in section 3, a complex flow field is apparent for the shrouded tail rotor. After implementation of a respective model in VAST, the results gathered with an open tail rotor model presented in this paper can be reviewed for their transferability to shrouded rotors. In the course of the project eTail, ground tests of an electric anti-torque system shall be conducted, the results of which can be used for validation of the models presented here as well as the shrouded tail rotor model.

9. ACKNOWLEDGMENTS

The work presented in this paper was funded by the German Federal Ministry for Economic Affairs and Climate Action under support code 20M1911E. The responsibility for the content of this paper lies with the authors.

Supported by:

Federal Ministry
for Economic Affairs
and Climate Action

on the basis of a decision
by the German Bundestag

The authors would like to thank the whole eTail team and especially Dr. Arnold and Mr. Stoll from ZFL for the fruitful discussions during the investigations. Thanks also go to the whole VAST development team for the support in the development activities and the ongoing extension of the modeling capabilities of VAST.

References

[1] R.D. Leoni. *Black Hawk: The Story of a World Class Helicopter*. American Institute of Aeronautics and Astronautics, Inc., 2007.

[2] M.G. Rozhdestvenskiy and A.P. Vaintrub. Tilted Tail Rotor Advantages and Problems to Solve. In *27th European Rotorcraft Forum*, Moskow, RU, September 2001.

[3] Bell Helicopter Textron Inc. Electric Distributed Propulsion Anti-torque Redundant Power and Control System. US patent US10526085B2, 2017.

[4] M. Stoll, U.T.P. Arnold, C. Hupfer, C. Stuckmann, S. Bichlmaier, M. Mindt, S. Seher-Weiß, S. Hibler, and F. Thielecke. Full Electric Helicopter Anti-Torque.

In *48th European Rotorcraft Forum*, Winterthur, CH, September 2022.

[5] Kopter Group. Official website, media section. https://koptergroup.com/media/, 2021. Accessed: 2021-10-06.

[6] J. Hofmann, M. Kontak, M. Mindt, and F. Weiß. VAST - Versatile Aeromechanics Simulation Platform for Helicopters. In *Deutscher Luft- und Raumfahrtkongress 2020*, Aachen, G, September 2020.

[7] E. Alpman, L.N. Long, and B.D. Kothmann. Toward a Better Understanding of Ducted Rotor Antitorque and Directional Control in Forward Flight. In *American Helicopter Society 59th Annual Forum*, Phoenix, AZ, May 2003.

[8] G. D. Padfield. *Helicopter Flight Dynamics, Chapter 3*. Blackwell Publishing, 2nd edition, 2007.

[9] D. M. Pitt and D. A. Peters. Theoretical Predictions of Dynamic Inflow Derivatives. *Vertica*, vol. 5, pp. 21–34, 1981.

[10] H. Glauert. A General Theory of the Autogyro. Technical Report ARC R&M 1111, 1926.

[11] D. Han and G.N. Barakos. Variable Speed Tail Rotors for Helicopters with Variable Speed Main Rotors. *Aeronautical Journal*, 121(1238):433–448, April 2017.

[12] C. Tung, J.C. Erickson, and F.A. DuWaldt. The Feasibility and Use of Anti-Torque Surfaces Immersed in Helicopter Rotor Downwash. Technical Report CAL No. BB-258-S-2, Cornell Aeronautical Lab, 1970.

[13] H. Schlichting and E. Truckenbrodt. *Aerodynamik des Flugzeugs 2. Band, Chapter 7*. Springer Verlag Berlin Heidelberg, 3rd edition, 2001.